Rare Metal Materials and Engineering
Volume 51, Issue 2, February 2022
Available online at www.rmme.ac.cn

Science Press

Cite this article as: Wang Qingjuan, Fan Ruixue, Liu Dan, et al. Microstructure and Properties of Graphene-Reinforced Cu-Cr-Zr Matrix Composites Fabricated by Spark Plasma Sintering[J]. Rare Metal Materials and Engineering, 2022, 51(02): 414-421.

ARTICLE

Microstructure and Properties of Graphene-Reinforced Cu-Cr-Zr Matrix Composites Fabricated by Spark Plasma Sintering

Wang Qingjuan, Fan Ruixue, Liu Dan, Zhang Yufeng, Wang Wei, Du Zhongze, Liu Shifeng

Xi'an University of Architecture and Technology, Xi'an 710055, China

Abstract: Copper matrix composites reinforced with graphene nanoplatelets (GNPs) were prepared by low-energy ball milling and spark plasma sintering (SPS). The effects of graphene content on the microstructure and the properties of such composites were studied. The results show that as the graphene content increases, the mechanical properties of the composite first improve and then gradually deteriorate. When the graphene content is 0.25wt%, the ultimate compressive strength of the composite is 409 MPa and its electrical conductivity is as high as 90% International Annealed Copper Standard (IACS). Further addition of graphene in the composite produces a larger cluster of GNPs within the copper matrix and results in the deterioration of the aforementioned properties. However, as the graphene content continues to increase, the wear rate of the composite declines steadily. The uniform distribution of graphene amongst the copper particles enables the transformation of the external applied load from the copper matrix to the chromium particles and graphene, effectively blocking internal dislocation motion, and thus improving the strength and other tribological properties of the composites.

Key words: graphene/Cu-Cr-Zr alloy; ball milling; spark plasma sintering; microstructure; mechanical properties

Cu-Cr-Zr alloy has excellent thermal conductivity and moderate strength, and is an important engineering structural material for high-speed railway contact wires, lead frames, and electrical resistance welding electrodes[1-3]. Electrical conductivity, strength, and wear resistance are the three noteworthy properties that allow this alloy to be used in such crucial applications. However, the electrical conductivity and strength of the alloy are difficult to reconcile, causing a significant hindrance in the improvement of the performance of this alloy[4,5]. Adding a second phase into the copper matrix is an effective work-around method to enhance the properties of the alloy[6,7].

Graphene has a large surface area, excellent mechanical properties, and exceptional electrical and thermal conductivity. Over the past few years, it has been successfully used to prepare metal matrix composites[8]. In this study, graphene was introduced into a copper matrix and dispersed into the matrix by chemical mixing, mechanical mixing, and electrode deposition[9,10] techniques. Zhang et al[11] fabricated graphene/carbon fiber copper matrix composites by a hot-pressing process. Chen et al[12] synthesized these copper-based composites via a molecular-level mixing process. On the one hand, it is found that the addition of graphene causes a decrease in the electrical conductivity of the composites due to the dispersion of graphene in the matrix during the transmission process. On the other hand, an increase in graphene content causes an improvement in the tensile strength of the composites, even though it reduces the plasticity. The compromised plasticity can be attributed to the poor wettability between graphene and the copper matrix, resulting in a weak interface bond between them. Since studies have shown that the addition of alloy components can

---

Received date: February 08, 2021
Foundation item: International Science and Technology Cooperation Project of Shaanxi Province, China (2019KW-064); Shaanxi Provincial Department of Education 2019 Annual Service for Local Science Research Project (19JC025)

Corresponding author: Wang Qingjuan, Ph. D., Professor, School of Metallurgical Engineering, Xi'an University of Architecture and Technology, Xi'an 710055, P. R. China, E-mail: jiandawqj@163.com

Copyright © 2022, Northwest Institute for Nonferrous Metal Research. Published by Science Press. All rights reserved.

optimize copper matrix composites. Chu et al[13] used pre-alloyed CuCr powder to prepare reduced graphene oxide (RGO)/CuCr composites, the strength of which was attributed to the formation of Cr_7C_3 nanoparticles. Subsequently, Zhang et al[14] also studied the effect of different percentages of chromium content on graphene copper-based composites, because although extensive studies have been conducted on various aspects of graphene/copper matrix composites, few studies researched the effect of addition of chromium and zirconium on the copper matrix. It is observed that the addition of chromium is conducive to strengthening the copper matrix. At the same time, the addition of graphene has been proven to reduce the electrical conductivity of the alloy[15,16]. Achieving a favorable relationship between the constitution of the composites and their physical properties thus becomes the prime focus of this study. Studying the micro-mechanism of graphene-reinforced copper matrix composites and optimizing them via alloy components are the key to understand graphene-reinforced copper matrix composites.

In this study, GNP/Cu-Cr-Zr composites were prepared via low-energy ball milling and spark plasma sintering (SPS) processes. Graphene dispersion in the matrix and the effect of graphene content on the properties of GNP/Cu-Cr-Zr composites were studied.

1 Experiment

The primary materials used in this study were custom-made copper (Cu) powder, chromium (Cr) powder, and zirconium (Zr) powder, all of 99.9% purity. The schematic of the fabrication process of GNP/Cu-Cr-Zr composite is shown in Fig.1. In the first step, 1wt% Cr powder, 0.1wt% Zr powder, and 98.9wt% Cu powder were weighed and put into a planetary ball milling machine for 6 h, where the mass ratio of the powder was 3:1 and the milling speed was 300 r/min. In the second step, the powdered mixture of Cu-Cr-Zr and graphene with different mass fractions were ball milled again for 8 h. The mixed Cu-Cr-Zr powders with 0, 0.25wt%, 0.5wt%, 0.75wt%, and 1wt% graphene were named as Cu-Cr-Zr, 0.25%GNP/Cu-Cr-Zr, 0.5%GNP/Cu-Cr-Zr, 0.75%GNP/Cu-Cr-Zr, and 1%GNP/Cu-Cr-Zr composites, respectively. In the third step, the mixed powders were sintered using SPS (Germany FCT D25/3) at 800 °C and 30 MPa for 5 min. The as-sintered samples were each 40 mm in diameter and 10 mm in thickness.

The microstructure of the powder and composites was studied under a scanning electron microscopic (SEM, Gemini 300). The structure and phase of the powder and composites were analyzed by X-ray diffraction (XRD, D8 ADVANCE A25). The hardness was tested by a 401MVD Vickers hardness tester, with a load of 50 g and a loading time of 10 s, and five points were used for each sample to obtain the average value. The electrical conductivity of the sample was measured by an eddy-current conductivity meter (7501). The room temperature compression test was performed on a 1314 Instron testing machine with a strain rate of 0.5 mm/min. The tribological test was conducted at room temperature using a ball-on-disk multifunctional tribometer. A 2.5 mm diameter GCr15 ball was selected as the friction pair material and reciprocated at a stroke distance of 5 mm. The applied load and sliding speed were maintained at 500 g and 200 r/min, respectively. The duration of the test was 30 min. Each test was repeated three times, and the average value was recorded.

2 Results and Discussion

2.1 Microstructure

The SEM images of the preliminary Cu, Cr and Zr powders, and the morphologies of graphene are shown in Fig. 2. Fig. 2a reveals that the Cu powder has large agglomerates with an average size of 75 μm and is irregularly shaped. As shown in Fig. 2b and 2c, the Cr and Zr powders have no such irregularly shaped agglomerates but have flat ones instead, with an average size of 45 μm. Fig.2d shows the morphology of the graphene nanoplatelets (GNPs) which are crumpled sheet-like structures with 0.5~5 μm in lateral width and 0.8 nm in thickness.

The SEM morphologies and XRD patterns of mixed composite powders are shown in Fig.3. GNPs were spread out and homogeneously distributed between the copper particles (Fig. 3b). There are many wrinkles on the surface of these copper particles, so graphene is embedded in each wrinkle after ball milling to achieve an even distribution. The XRD pattern of the composite powders is shown in Fig.3c. Only the

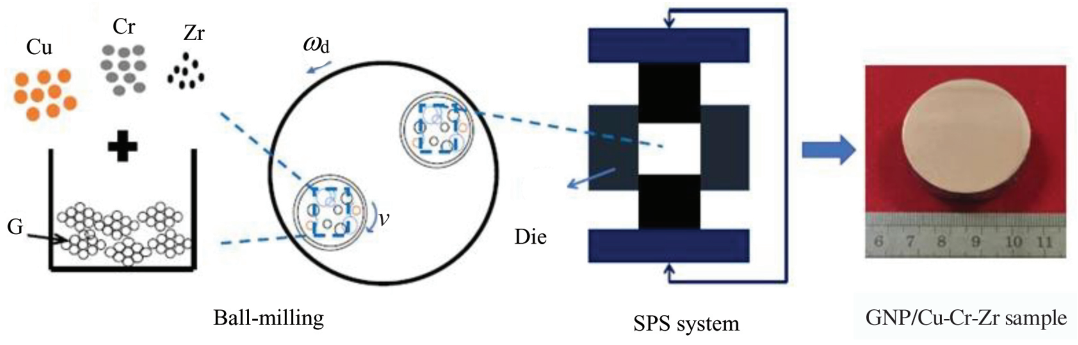

Fig.1 Schematic of fabrication process of GNP/Cu-Cr-Zr composites

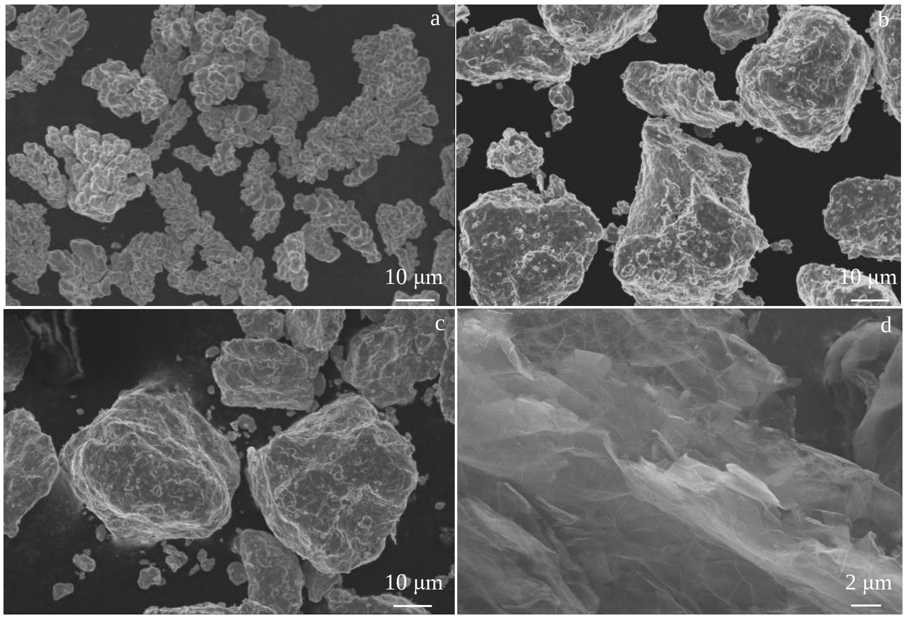

Fig.2 SEM morphologies of Cu (a), Cr (b) and Zr (c) powders used as the raw materials and morphology of graphene (d)

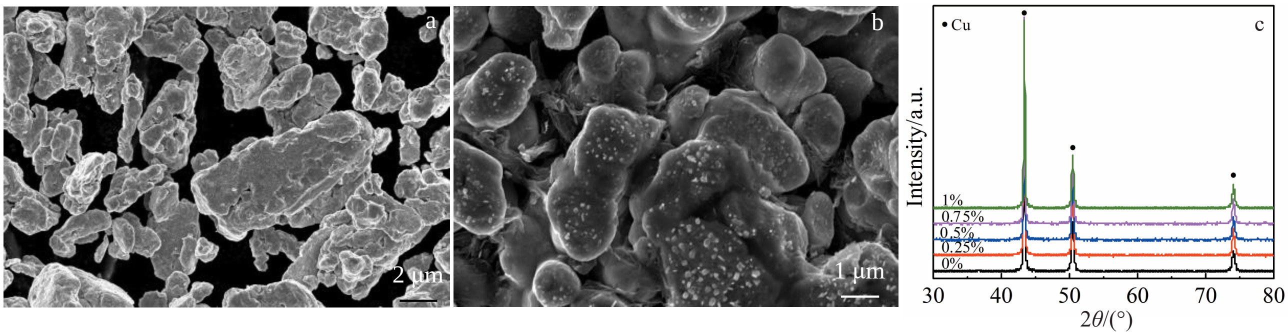

Fig.3 SEM morphologies of Cu-Cr-Zr powders (a) and Cu-Cr-Zr powders with 0.5% GNP distributed on the surface (b); XRD patterns of composite powders with different graphene contents (c)

diffraction peaks of face-centered cubic (fcc) Cu phase are found, and no other newly-generated intermetallic compounds appear. The characteristic peaks of graphene, Cr, and Zr phases are not detected in the mixed powder, which may be due to their relatively low content. The XRD patterns of alloys with different graphene contents after sintering are shown in Fig. 4. After sintering, several groups of composites have Cu diffraction peaks. In addition, Cu and Cr produce two compounds, Cu_8Zr_3 and $Cu_{10}Zr_7$ when sintered at 800 °C.

SEM images of the sintered bulk composites and EDS spectrum of Cr, GNP are shown in Fig.5. From Fig.5a and 5d, it is observed that Cr particles are present separately and uniformly distributed in the copper matrix. A small amount of graphene is added and banded in the copper matrix. For further characterization of the GNP, Cr, and Zr, the metallographic sample of the 0.5wt% GNP/Cu-Cr-Zr composite was corroded by concentrated nitric acid to remove the Cu matrix. The morphology after corrosion is shown in Fig. 6. Fig. 6b shows that the GNP after sintering still appears in a folded layer form. The energy dispersive spectrometer (EDS) mapping further corroborates the uniform distribution of GNP. Meanwhile, Cr and Zr also appear after corrosion. This confirms the presence of Cr, Zr and graphene in the composite.

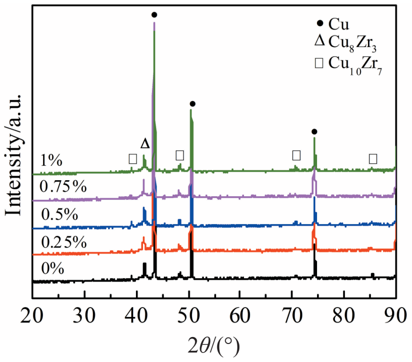

Fig.4 XRD patterns of composites with different graphene contents

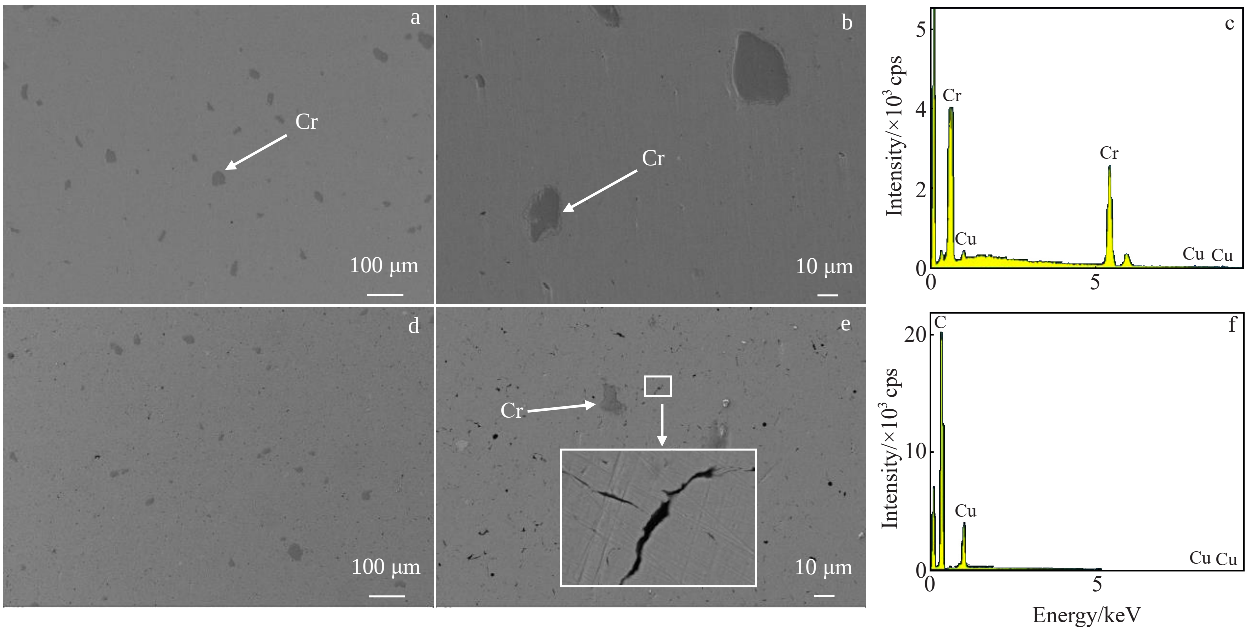

Fig.5 SEM images of the sintered bulk composites: (a, b) Cu-Cr-Zr and (d, e) 0.5wt%GNP/Cu-Cr-Zr composite; EDS spectra of Cr (c) and GNP (f)

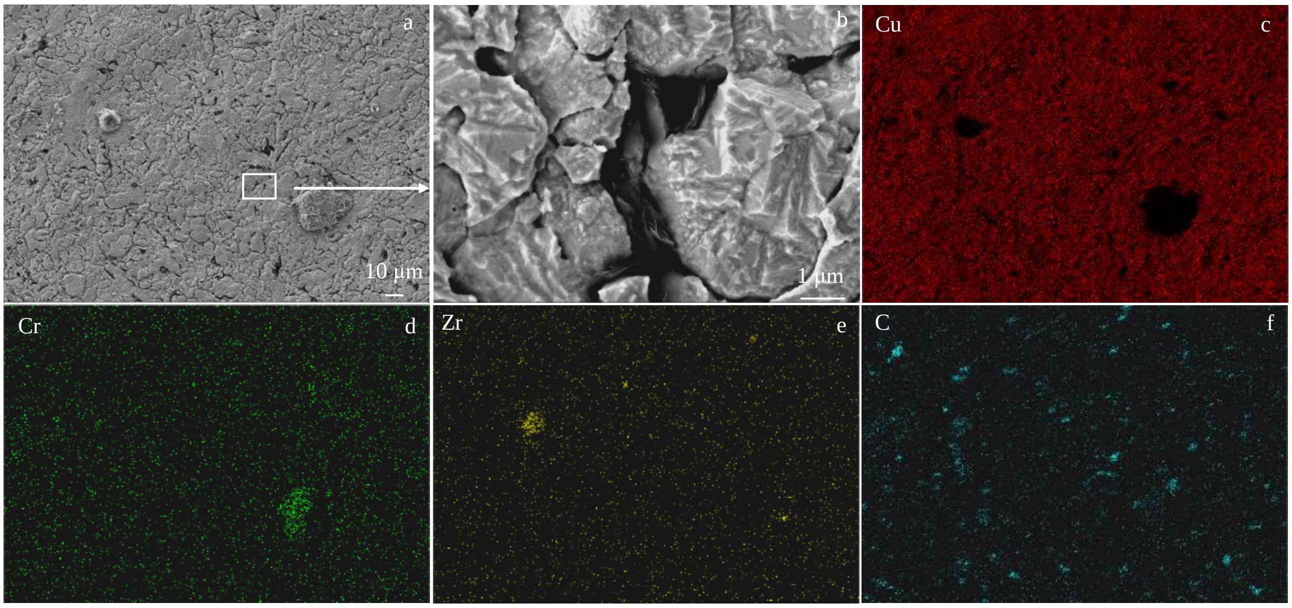

Fig.6 SEM morphologies of exposed GNP, Cr and Zr in etched GNP/Cu-Cr-Zr composite (a) and higher magnification image of GNP (b); EDS mapping of element Cu (c), Cr (d), Zr (e), and C (f)

2.2 Electrical conductivity and hardness of the sintered bulk composite

The electrical conductivity and hardness of the sintered bulk composites are both shown in Fig. 7. The electrical conductivity of the GNP/Cu-Cr-Zr composites is lower than that of pure Cu-Cr-Zr, which is similar to the observations for Cu alloys reinforced with GNP, as reported by Chen et al[12]. The electrical conductivity of the composites has various degrees of decline upon addition of graphene. The overall conductivity does not drop much and in fact, the conductivity of the 1wt%GNP/Cu-Cr-Zr composite can even surpass 80% IACS. This shows that the electrical conductivity of these composites depends not only on their graphene content, but also on their defect density. The powder sintering process produces a composite that is not particularly dense due to the presence of pores within the structure. These pores significantly reduce the resistivity of the composite. The dispersion of graphene among the copper particles implies

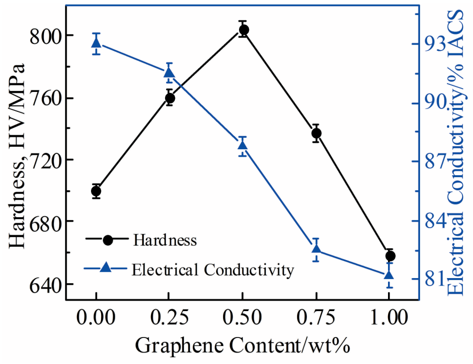

Fig.7 Electrical conductivity and hardness of the composites

that electrons are transmitted in both directions across the copper “grain”/graphene interface, and this scattering of electrons causes a reduction in the conductivity of the composite. Increase in graphene content in the composites also affects the hardness, which first increases and then decreases. The incorporation of GNP into the Cu-Cr-Zr alloy causes the hardness to increase from 700 MPa to a maximum value of 820 MPa. However, when the graphene content exceeds 0.5wt%, the hardness decreases sharply.

This behaviour can be attributed to the inherent load bearing strength of graphene, as well as the way it is dispersed in the matrix; when the graphene content is low, it is uniformly distributed throughout the matrix and has good interfacial bonding with it. These characteristics help to inhibit any grain growth, thus impeding any dislocation movement. However, when the graphene content exceeds 0.5wt%, the dispersion of graphene in the matrix becomes more difficult and causes local agglomeration, resulting in an uneven overall distribution. Therefore, a reasonable control over the graphene content contributes to excellent performance of the composite material.

2.3 Mechanical properties

The compressive stress-strain curves of GNP/Cu-Cr-Zr composites at room temperature are shown in Fig. 8a. The 0.25%GNP/Cu-Cr-Zr composite shows a compressive yield strength of 172 MPa and an ultimate compressive strength of 409 MPa, both of which are 40% and 13% higher than the values for Cu-Cr-Zr, respectively. The addition of graphene increases the overall yield stress of the material.

Graphene can be used as an effective reinforcing agent, and it is also a key factor affecting the mechanical properties of these composites. When the graphene content is low, the ball milling process can uniformly disperse the graphene in the matrix. In such a situation, when the composite is subjected to external force, the graphene acts as a medium for transmitting stress, giving the composite material excellent compressive strength. Fig. 8b shows the strengthening effect of different metal matrix composites. The formula of strengthening efficiency is shown in Eq. (1), and the relation between the volume fraction (V_r) and mass fraction (W_r) of the reinforcement of composite is shown in Eq.(2)[17]:

$$R = \frac{\sigma_c - \sigma_m}{V_r \sigma_m} \tag{1}$$

$$V_r = \frac{W_r \rho_m}{W_r \rho_m - (1 - W_r) \rho_r} \tag{2}$$

where R is the reinforcing efficiency, σ_c is the yield strength of the composite, σ_m is the yield strength of the matrix, and ρ_r and ρ_m are the density of the graphene reinforcement and matrix, respectively. It is shown that the enhancement efficiency of graphene in Cu/GNP composites prepared by this method is better than that observed in Ref.[18-22,14]. For copper-based composites, the R-value of GNP or graphene oxide (GO) is higher than that of carbon nanotubes (CNT), because graphene has a higher strength and a larger specific surface area[17]. The strength enhancement of GNP/Cu-Cr-Zr composite is attributed to the strengthening of GNPs with homogeneous dispersion and complete structure.

To further observe the deformation evolution of the GNP/Cu-Cr-Zr composites, the deformed structure of the 0.5wt% GNP/Cu-Cr-Zr composite is shown in Fig. 9 (the dark arrows indicate the compressive axis). Parallel graphene streaks are found in the composite after compression and further observation also shows bending of the graphene around the Cr particles. The hard Cr particles are uniformly distributed in the matrix (Fig. 5a). The load is thus transferred from the copper matrix to the Cr particles, which improves the strength. However, research on graphene-reinforced metal matrix composites has shown that the main reinforcement mechanisms are dislocation enhancement and stress transfer[23-26]. For the RGO/Cu-Cr composites as prepared by

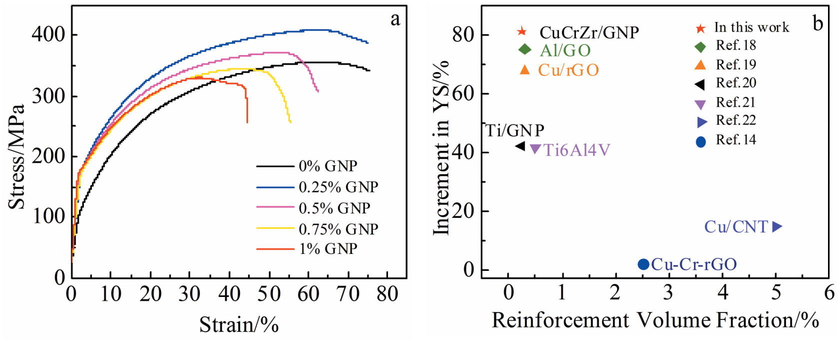

Fig.8 Compressive stress-strain curves of the sintered bulk composites (a) and strengthening efficiency of different materials (b)

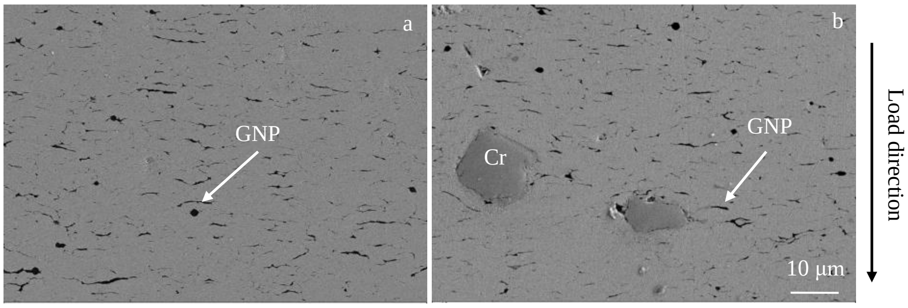

Fig.9 SEM images of the room-temperature deformed 0.5wt%GNP/Cu-Cr-Zr composite: (a) banded GNP agglomeration and (b) deformed GNP around Cr particles

Chu et al[13], the computational results showed that the interfacial shear strength is increased by 62%, indicating that the load transfer effect is the most effective one in the reinforcement mechanism. This is conclusive that graphene can effectively block the internal dislocations by itself in the composite and aid in the load transfer from the matrix to the filler.

2.4 Tribological performance of composites

The average friction coefficient and wear rate of sintered Cu-Cr-Zr composites with different graphene contents are shown in Fig. 10. The average friction coefficient of both 0.25%GNP/Cu-Cr-Zr and 0.5%GNP/Cu-Cr-Zr composites is approximately 0.7 and 0.62, respectively. The addition of even a small amount of graphene cannot particularly improve the abrasion resistance. However, the friction coefficient sharply decreases when the graphene content is further increased. The friction coefficient of composite with 0.75wt% graphene is about 0.25, which is 60% lower than that of Cu-Cr-Zr. This shows that the addition of graphene has a certain anti-friction effect on the composite. An increase in graphene content also has an inversely proportional effect on the wear rate of the composite, decreasing from 5.35×10^{-6} mm^3/(N·m) to 1.5×10^{-6} mm^3/(N·m). The wear rate of a material is a synergistic effect of its wear resistance and mechanical properties, implying that as the graphene content increases, the mechanical properties of the alloy decrease. Nonetheless, compared to the reduction in mechanical properties, a reduction in the friction coefficient contributes more to the wear resistance of an alloy, thus explaining the declining wear rate of composites.

The SEM morphology of the worn surface is shown in Fig.11. As observed from Fig.11a, the surface of the wear scar is relatively rough, with obvious furrows and cutting morphology. The primary wear mechanism on the Cu-Cr-Zr surface is abrasive wear, which is also the reason for the highest wear rate amongst the fabricated composites. Since the hardness of Cu-Cr-Zr is quite different from that of the friction pair steel balls, the latter accumulates a large amount of Cu debris in furrows on the surface during the friction test. The friction surface gradually changes from the original Cu-Fe wear to Cu-Cu wear, resulting in a higher friction coefficient and wear rate of the Cu-Cr-Zr composite.

The 0.25%GNP/Cu-Cr-Zr composite wear track has a width of approximately 1897 μm and a severely coarse surface with large wear debris. In this case, the main wear mechanism of the alloy is adhesive wear. Plastic deformation occurs along with frictional wear and the graphene particles are exposed on the contact surface. When plastic deformation of the contact surfaces is prevented, the wear rate of the material can be minimized[27]. Under normal load, graphene and metal filings usually get compacted to form a thin friction layer on the contact surface. However, for composite materials with 0.25wt% graphene, there are fewer graphene particles on the surface and in turn fewer deficit during frictional wear. Since the abrasive adhesion is strong and the surface area susceptible to damage is large during sliding, the 0.25%GNP/Cu-Cr-Zr composite yields the highest coefficient of friction. As the

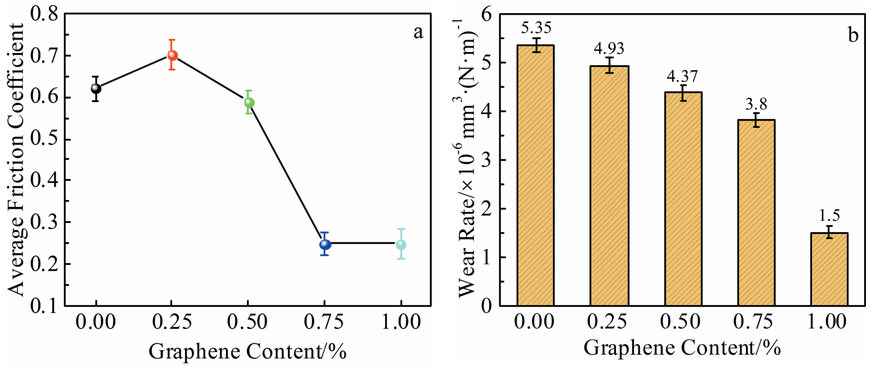

Fig.10 Tribological properties of composites: (a) average friction coefficient and (b) wear rates

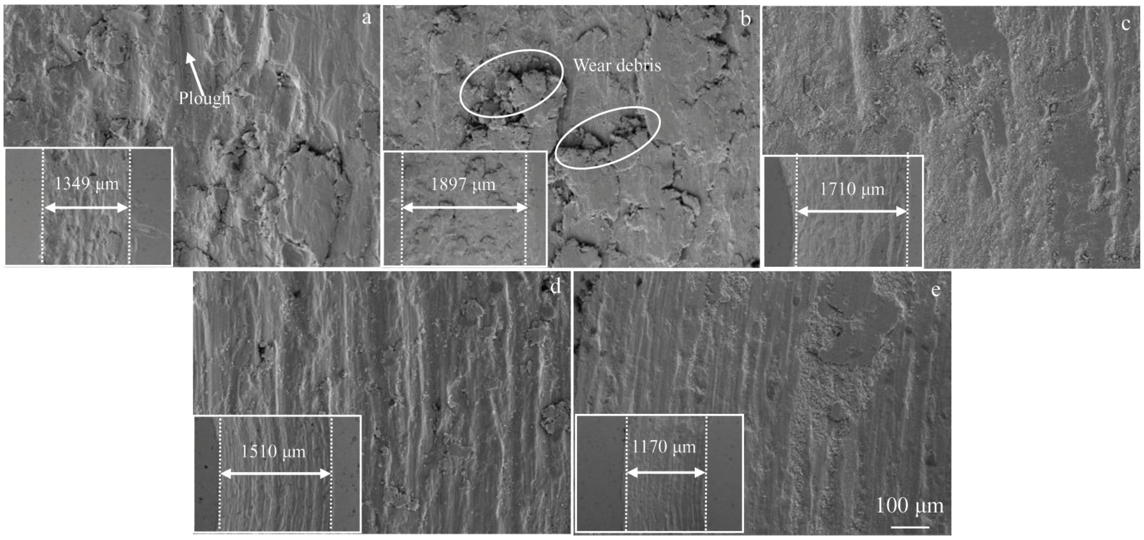

Fig.11 SEM morphologies of worn surface of composites: (a) Cu-Cr-Zr, (b) 0.25%GNP/Cu-Cr-Zr, (c) 0.5%GNP/Cu-Cr-Zr, (d) 0.75%GNP/Cu-Cr-Zr, and (e) 1%GNP/Cu-Cr-Zr (insets are their corresponding low magnification images, showing the width of the wear track)

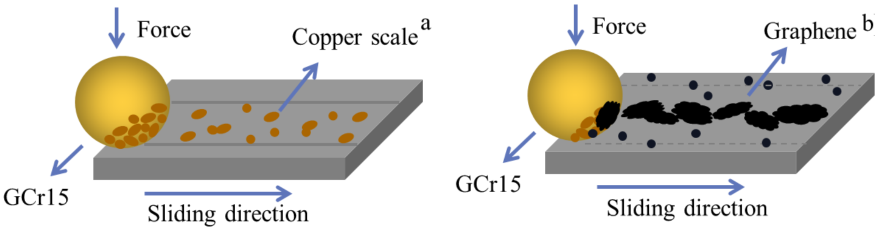

Fig.12 Wear mechanism of Cu-Cr-Zr (a) and GNP/Cu-Cr-Zr (b)

graphene content continues to increase, the width of the wear scar continues to decrease. From Fig. 11c~11e, it shows that the wear surface becomes smoother and flatter, without a large amount of accumulated debris. Subsequently, when compared to the 0.25%GNP/Cu-Cr-Zr composite, the wear surface of 1%GNP/Cu-Cr-Zr composite is quite flat, but still has a small amount of fine wear marks.

The change of wear mechanism is shown in Fig. 12. In the friction process between Cu-Cr-Zr alloy and steel ball, a large number of Cu chips in the furrow adhere to the surface of the alloy, and the friction surface gradually changes from the original Cu-Fe wear to Cu-Cu wear, as shown in Fig. 12a, which leads to the high friction coefficient and wear rate of Cu-Cr-Zr alloy. The wear mechanism of the Cu-Cr-Zr alloy is abrasive wear. As shown in Fig. 12b, when graphene is added into the composites, it can be spread out on the surface of the composites during the friction process. This can reduce the friction coefficient of the composites. With the further increase of graphene content, more graphene will be exposed to the contact surface. And the graphene film on the worn surface becomes relatively continuous. An anti-wear layer is formed on the worn surface and the friction coefficient decreases continuously. The wear mechanism of the composites changes into adhesion wear.

3 Conclusions

1) GNP/Cu-Cr-Zr composites with different graphene contents are prepared via SPS process. As grapheme content increases, the electrical conductivity of the composites continues to decrease, which can also reach 80% IACS or higher.

2) Graphene still retains a lamellar structure after sintering, indicating that this method does not particularly damage its structure and characteristics.

3) The addition of graphene can significantly increase the compressive yield strength of the composites. Overall, when the graphene content is 0.25wt%, the performance of the composite is the most desirable. The ultimate compressive strength of the 0.25%GNP/Cu-Cr-Zr composite reaches 409 MPa, increased by 13% as compared to that of Cu-Cr-Zr.

4) In regard to the friction performance, the addition of graphene can evidently reduce the friction coefficient from 0.62 of Cu-Cr-Zr to about 0.25 of 1%GNP/Cu-Cr-Zr composite, indicating that the addition of graphene is beneficial for improving the wear resistance of the material.

References

1 Huang F X, Ma J S, Geng Z T *et al. Rare Metal Materials and*

Engineering[J], 2004, 33(3): 267
2 Dong B W, Zhong S J, Pei Y Y *et al*. *Rare Metal Materials and Engineering*[J], 2020, 49(12): 4081 (in Chinese)
3 Chen X H, Zhou H L, Zhang T *et al*. *Mater Des*[J], 2019, 180: 107 976
4 Zhang Y, Volinsky A A, Tran H T *et al*. *J of Materi Eng Perform* [J], 2015, 24: 3783
5 Li J, Chang L, Li S *et al*. *Journal of Rare Earths*[J], 2018, 36(4): 424
6 Fang Q, Kang Z, Gan Y *et al*. *Materials & Design*[J], 2015, 88: 8
7 Zhou J, Zhu D, Tang L *et al*. *Vacuum*[J], 2016, 131: 156
8 Kinloch I A, Suhr J, Lou J *et al*. *Science*[J], 2018, 362: 547
9 Ponraj N V, Azhagurajan A, Vettivel S C *et al*. *Surfaces and Interfaces*[J], 2017, 6: 190
10 Chen X F, Tao J M, Yi J H *et al*. *Materials Science & Engineering A*[J], 2018, 718: 427
11 Zhang X J, Yang W C, Zhang J Y *et al*. *Materials Science & Engineering A*[J], 2019, 743: 512
12 Chen F, Ying J, Wang Y *et al*. *Carbon*[J], 2016, 96: 836
13 Chu K, Wang F, Li Y B *et al*. *Carbon*[J], 2018, 133: 127
14 Zhang X J, Dai Z K, Liu X R *et al*. *Acta Metallurgica Sinica*[J], 2018, 31(7): 761
15 Hamedan S, Abdi M, Sheibani S. *Chinese Journal of Nonferrous Metals*[J], 2018, 28: 2044 (in Chinese)
16 Uchida S, Kimura T, Nakamoto T *et al*. *Materials & Design*[J], 2019, 175: 107 815
17 Hidalgo-Manrique P, Lei X, Xu R *et al*. *J Mater Sci*[J], 2019, 54: 12 236
18 Wu Y H, Zhan K, Yang Z *et al*. *Journal of Alloys and Compounds*[J], 2019, 775: 233
19 Jiang R, Zhou X, Fang Q *et al*. *Materials Science & Engineering A*[J], 2016, 654: 124
20 Liu J, Wu M, Yang Y *et al*. *Journal of Alloys and Compounds*[J], 2018, 765: 1111
21 Li A, Shi L, Zhang W *et al*. *Materials Letters*[J], 2019, 257: 126 750
22 Nayan N, Shukla A. K, Chandran P *et al*. *Materials Science & Engineering A*[J], 2017, 682: 229
23 Xiong D B, Cao M, Guo Q *et al*. *ACS Nano*[J], 2015, 9: 6934.
24 Hwang J, Yoon T, Jin S H *et al*. *Adv Mater*[J], 2013, 25(46): 6724
25 Yang Z Y, Wang L D, Cui Y *et al*. *Nanoscale*[J], 2018, 10: 16 990
26 Zhang D D, Zhan Z J J. *Journal of Alloys and Compounds*[J], 2016, 658: 663
27 Li J F, Zhang L, Xiao J K *et al*. *Transactions of Nonferrous Metals Society of China*[J], 2015, 25(10): 3354

放电等离子烧结法制备石墨烯-铜铬锆合金的组织与性能

王庆娟，樊瑞雪，刘　丹，张玉峰，王　伟，杜忠泽，刘世锋
(西安建筑科技大学，陕西 西安 710055)

摘　要：采用低能球磨和放电等离子烧结法制备了石墨烯（GNPs）增强铜基复合材料。研究了石墨烯含量对复合材料微观结构和性能的影响。结果表明，随着石墨烯含量的增加，复合材料的力学性能呈现出先升高后降低的趋势。其中，当石墨烯含量为0.25%（质量分数）时，复合材料的极限抗压强度为409 MPa，合金的导电率高达90% IACS。石墨烯含量的增加导致其在铜基体中的团聚现象严重。此外，随着石墨烯含量的增加，合金的磨损率不断下降。石墨烯的加入显著改善了摩擦性能。屈服强度的增加是由于石墨烯在铜基体中的均匀分布。同时，载荷从铜基体转移到铬颗粒和石墨烯中，有效地阻碍了位错运动。

关键词：石墨烯-铜铬锆合金；球磨；放电等离子烧结；组织结构；力学性能

作者简介：王庆娟，女，1973年生，博士，教授，西安建筑科技大学冶金工程学院，陕西 西安 710055，E-mail：jiandawqj@163.com